EJN fens European Journal of Neuroscience

European Journal of Neuroscience, Vol. 32, pp. 932–938, 2010 doi:10.1111/j.1460-9568.2010.07393.x

MOLECULAR AND DEVELOPMENTAL NEUROSCIENCE

Cellular & molecular Ca^{2+} microdomains in olfactory cilia support low signaling amplification of odor transduction

Karen Castillo,[1,2] Diego Restrepo[3] and Juan Bacigalupo[1,2]
[1]Department of Biology, Faculty of Sciences, University of Chile, Santiago, Las Palmeras 3525, Ñuñoa, Santiago 7800024, Chile
[2]Millennium Institute for Cell Dynamics and Biotechnology, University of Chile, Santiago, Chile
[3]Department of Cell and Developmental Biology and Neuroscience Program, University of Colorado Denver, CO, USA

Keywords: Ca^{2+} fluorescence, calcium, cyclic nucleotide-gated channels, microdomains, odor transduction, olfactory neuron

Abstract

Signal transduction depends critically on the spatial localization of protein constituents. A key question in odor transduction is whether chemotransduction proteins organize into discrete molecular complexes throughout olfactory cilia or distribute homogeneously along the ciliary membrane. Our recordings of Ca^{2+} changes in individual cilia with unprecedented spatial and temporal resolution, by the use of two-photon microscopy, provide solid evidence for Ca^{2+} microdomains (transducisomes). Dissociated frog olfactory neurons were preloaded with caged-cAMP and fluo-4 acetoxymethyl ester probe Ca^{2+} indicator. Ca^{2+} influx through cyclic nucleotide-gated (CNG) channels was evoked by uniformly photoreleasing cAMP, while ciliary Ca^{2+} was measured. Discrete fluorescence events were clearly resolved. Events were missing in the absence of external Ca^{2+}, consistent with the absence of internal Ca^{2+} sources. Fluorescence events at individual microdomains resembled single-CNG channel fluctuations in shape, mean duration and kinetics, indicating that transducisomes typically contain one to three CNG channels. Inhibiting the Na^+/Ca^{2+} exchanger or the Ca^{2+}-ATPase prolonged the decay of evoked intraciliary Ca^{2+} transients, supporting the participation of both transporters in ciliary Ca^{2+} clearance, and suggesting that both molecules localize close to the CNG channel. Chemosensory transducisomes provide a physical basis for the low amplification and for the linearity of odor responses at low odor concentrations.

Introduction

Odor transduction takes place in the cilia of the sensory neurons of the olfactory epithelium. Odor binding to specific receptors triggers a G_{olf}-mediated cascade, in which activation of adenylyl cyclase III raises the cAMP concentration. This nucleotide directly gates ciliary cyclic nucleotide-gated (CNG) channels (Schild & Restrepo, 1998), mediating the influx of Ca^{2+} ions that elicit the opening of Ca^{2+}-activated Cl^- (Cl_{Ca}) channels. As the Cl^- concentration is higher in the ciliary lumen than in the external mucus, both channels contribute to cell depolarization (Kurahashi & Yau, 1993; Lowe & Gold, 1993). Intracellular Ca^{2+} also plays a key role in olfactory adaptation, largely by decreasing CNG channel affinity for cAMP (Chen & Yau, 1994).

Olfactory cilia (< 0.2 μm in diameter, 5 μm to a few 100 μm long, depending on the species) are devoid of internal organelles (Menco, 1992), making the extracellular milieu the only source and sink of Ca^{2+}. In the ciliary membrane, an Na^+/Ca^{2+} exchanger (NCX) (Reisert & Matthews, 1998) and a plasma membrane Ca^{2+}-ATPase (PMCA) (Castillo *et al.*, 2007; Antolin *et al.*, 2010) are the transporters responsible for Ca^{2+} clearance. It is possible that Ca^{2+} increases are confined to the local microenvironment around individual CNG channels, as with other Ca^{2+}-permeant channels (Naraghi & Neher, 1997; Fakler & Adelman, 2008). Takeuchi & Kurahashi (2008) measured electrical responses of similar amplitude to identical cAMP increments evoked in separate micrometer-long segments of individual olfactory cilia, arriving at the conclusion that there was no interaction between adjacent segments of that size. On the other hand, Bhandawat *et al.* (2005) reported evidence that odor responses are composed of small elementary units, consistent with the notion that odor transduction is organized into small protein ensembles involving a remarkably low gain. Here, we have directly tested for the presence of the hypothetical submicrometer ciliary Ca^{2+} microdomains, whose spatial organization and relative location might be relevant for the dynamics and amplification of signal transduction.

Correspondence: Juan Bacigalupo, [1]Department of Biology, as above.
E-mail: bacigalu@uchile.cl

Received 11 June 2010, revised 23 June 2010, accepted 27 June 2010

Materials and methods

Isolation of olfactory sensory neurons

Adult frogs (*Rana pipiens*) were anesthetized by cooling on ice, killed by decapitation and pithed. All procedures were approved by the animal care and use committee of the University of Colorado Denver. Olfactory epithelia were removed, cut into small pieces (approximately 1 mm^2) and maintained for < 8 h at 4°C in frog Ringer's solution. To dissociate the cells, pieces of tissue were torn apart with fine tweezers, passed three times through a fire-polished Pasteur pipette and filtered through a 70-μm mesh (Falcon, BD

Biosciences, San Jose, CA, USA). The cells were allowed to settle on a number 0 coverglass coated with CellTAK (BD Biosciences, San Jose, CA, USA) to attach the cells, in order to avoid movement of the cilia.

Solutions

Normal Ringer's contained 115 mM NaCl, 2.5 mM KCl, 2 mM $CaCl_2$, 0.4 mM $MgCl_2$, 10 mM HEPES and 10 mM glucose (pH 7.5); 0-Ca^{2+} Ringer's contained 115 mM NaCl, 2.5 mM KCl, 0.4 mM $MgCl_2$, 10 mM HEPES, 1 mM EGTA (no Ca^{2+} added) and 10 mM glucose (pH 7.5); and Li^+-Ringer's contained 115 mM LiCl, 2.5 mM KCl, 2 mM $CaCl_2$, 0.4 mM $MgCl_2$, 10 mM HEPES and 10 mM glucose (pH 7.5). The PMCA blocker 5(6)-carboxyeosin diacetate, succinimidyl ester (CE) (50 μM; Molecular Probes, Eugene, OR, USA) was added to normal Ringer's when needed. Chemicals were purchased from Sigma Chemical (St Louis, MO, USA), unless otherwise specified.

Ca^{2+} measurements in olfactory cilia

Cells were preincubated at room temperature for 40 min in Ringer's solution supplemented with 10 μM fluo-4 acetoxymethyl ester probe (Fluo-4 AM) (Molecular Probes) and then washed twice (10 min each) with Ringer's solution. Cells were then incubated for at least 25 min prior to the experiment in extracellular solution supplemented with 250 μM cell-permeable caged-cAMP (4,5-dimethoxy-2-nitrobenzyl adenosine 3′,5′-cyclic monophosphate; Molecular Probes). Cilia presenting a straight segment of at least 5 μm were chosen for Ca^{2+} fluorescence measurements in line raster scan mode.

All measurements were made with a two-photon microscope (Zeiss; model LSM-510 NLO), equipped with a Ti:sapphire laser running at 795 nm, and a 40× or 63× water immersion objective. Fluo-4 AM emission was collected with 500–550-nm bandpass filters.

To uncage cAMP, we placed an optic fiber (250 μm in diameter) transmitting UV light flashes (0.5–1 ms) delivered from a xenon flash lamp system (JML-C2; Rapp Optoelectronic) directly under the coverglass that held the cells. The beam from the optic fiber was centered within the focal field, where the cell was positioned. A scan line was positioned along a straight segment of a cilium and scanned every 3 ms or less for 1–3 min, providing a measurement of Ca^{2+} fluorescence changes as a function of time and distance in a ciliary segment. Time resolution was similar, but not identical, throughout experiments, because it depended on the length of the segment examined, being higher for shorter segments than for longer ones (range 1.9–3.0 ms). The time resolution of our fluorescent recordings is comparable to that in previous studies on Ca^{2+}-permeant channels with the same fluorescent probe, under total internal reflection fluorescence microscopy (Shuai & Parker, 2005; Demuro & Parker, 2006). To test the possibility that transient fluorescence events could be artefacts of non-biological origin, we conducted line-scan fluorescence measurements in an external solution containing the fluorophore (in its cell-impermeant form) at a concentration (10 μM) that would result in emission of light with intensities in the same range as the fluorescence measured from the cells) and three different Ca^{2+} concentrations. These measurements gave a rather uniform fluorescence signal, completely devoid of transient events, strongly supporting the biological origin of the transient fluorescence signals recorded from the cilia.

Analysis of Ca^{2+} fluorescence measurements

The time course of transient Ca^{2+} signals was quantified over a particular region of the recording where a Ca^{2+} signal was evident. Normalized fluorescence ($\Delta F/F_i$) vs. time was plotted (Figs 1C and F and 2C and F). F_i was the basal average fluorescence intensity in the same ciliary segment before exposure of the cilium to the UV light flash, and ΔF was the fluorescence intensity at any time point minus F_i. The time at which the Ca^{2+} signal declined to half its peak value ($\tau_{0.5}$) was measured for each experimental situation.

To characterize the individual fluorescent events, a small zone where Ca^{2+} increments occurred was chosen (five pixels, approximately 0.15 μm of cilium) and the events were quantified before and after cAMP release. In order to differentiate significant Ca^{2+} signals from basal noise, a discriminating line was defined as two standard deviations (SDs) above the average value of the basal fluorescence preceding CNG channel activation. There was no ambiguity in sorting out the individual fluorescence events, because the magnitude of the Ca^{2+} signals was generally much higher than that of the baseline noise. Event durations and their spatial dimensions were measured, and their cumulative distribution histograms were plotted (Fig. 3). Additionally, histograms of fluorescence amplitudes of the events occurring along the cilium segment at a given time, as well as those taking place at a given spot on the cilium for the duration of the experiment, were made for all experimental conditions. Average durations of individual fluorescence events were expressed as mean ± SD. Differences between average values were obtained with SIGMAPLOT 10 (Systat Software, Point Richmond, CA, USA).

Results

We addressed the question of whether transduction-dependent Ca^{2+} increases in olfactory cilia take place in microdomains by examining whether discrete Ca^{2+} fluorescence increments are elicited by sudden, uniform cAMP increments in olfactory cilia. We used two-photon microscopy, which allows measurement of the spatio-temporal distribution of Ca^{2+} fluorescence increments with submicrometer and submillisecond resolution, with limited contributions from out-of-focus fluorescence and negligible photobleaching, in contrast to conventional confocal microscopy (Denk *et al.*, 1995; Denk & Svoboda, 1997). Olfactory neurons were preloaded with caged-cAMP and the Ca^{2+} indicator Fluo-4 AM. cAMP was photoreleased by a UV flash. Figure 1 illustrates representative experiments conducted with 2 mM Ca^{2+} (control; A–C) and with no external Ca^{2+} (D–F). Line-scan fluorescence measurements were made every 3 ms or less for 180 s, in straight segments of individual cilia (Fig. 1A and D, red arrows). Multiple fluorescence spots were observed (Fig. 1B) along the cilium segment (ordinate, d) during the recording time in control solution (abscissa, time), indicating prominent Ca^{2+} increments at well-defined spots along the cilium (see below). This is shown in further detail for different times along the experiment in the insets underneath the continuous fluorescence recording (Fig. 1B). In the experiment in Fig. 1, the relative fluorescence measured in an approximately 0.4-μm-long stretch of the cilium (Fig. 1B, black arrowhead) over the whole duration of the experiment increased following the UV flash, reached a peak at approximately 35 s, and subsequently decayed to the basal level, with a half-maximal time of 11 s [Fig. 1C; $\tau_{0.5} = 10.5 \pm 1.9$ s (mean ± standard error of the mean); $n = 11$ of 17 cells tested]. A similar experiment performed with cilia bathed in 0-Ca^{2+} Ringer's solution showed only a few fluorescence events (Fig. 1E and F; $n = 8$), as expected because

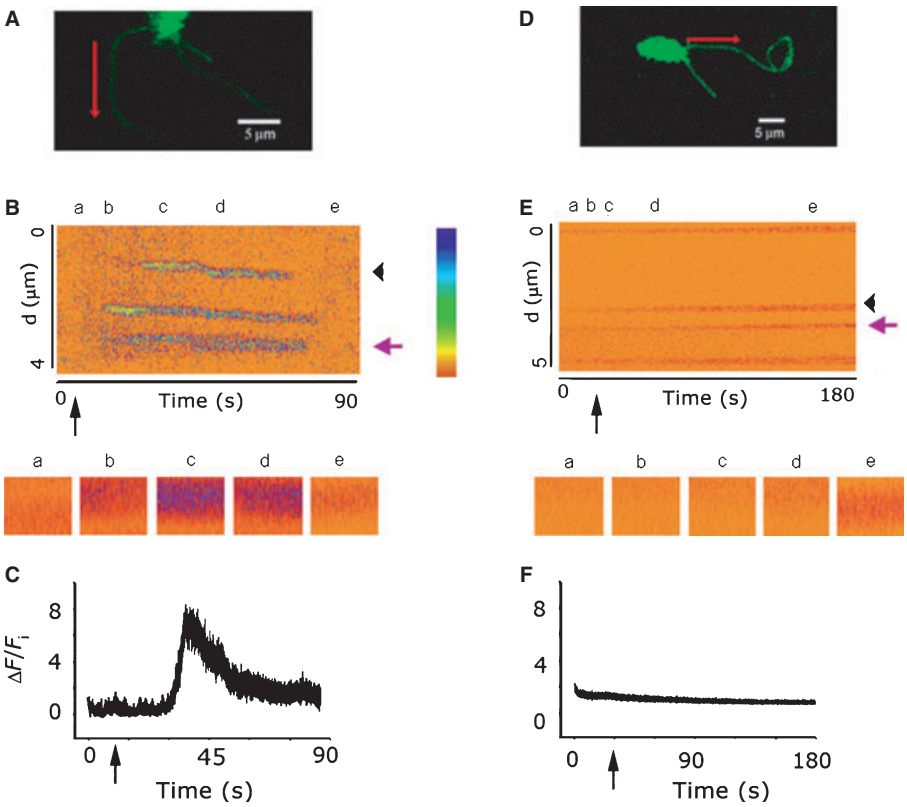

FIG. 1. Localized cAMP-induced Ca^{2+} increases in olfactory cilia. (A) Dendritic knob and cilia of an olfactory receptor neuron preloaded with Fluo-4 AM and caged-cAMP. The red arrow denotes the cilium segment from which the emission of fluorescence was collected and the direction of the scan. (B) Ca^{2+} fluorescence changes along the cilia segment; relative fluorescence intensity is color-coded, according to the calibration bar. The five insets underneath the fluorescence recording show details of it at the indicated ttimes (a–e). Black arrow: time of the photoreleasing UV flash. Violet arrow: ciliary segment from where insets were taken, at the times indicated by a–e. Black arrowhead: segment from where $\Delta F/F_i$ (C) was obtained. (C) Time course of the fluorescence change ($\Delta F/F_i$) for a selected ciliary region (black arrowhead in B). $\tau_{0.5}$ = 11 s. (D) Another olfactory neuron, bathed in 0-Ca^{2+} Ringer's solution. (E) Ca^{2+} fluorescence in the ciliary segment. (F) Relative fluorescence upon cAMP release. Labels as in A–C. Relative fluorescence was calculated by dividing fluorescence intensity by the average fluorescence intensity in the entire cilium for the period preceding cAMP photorelease.

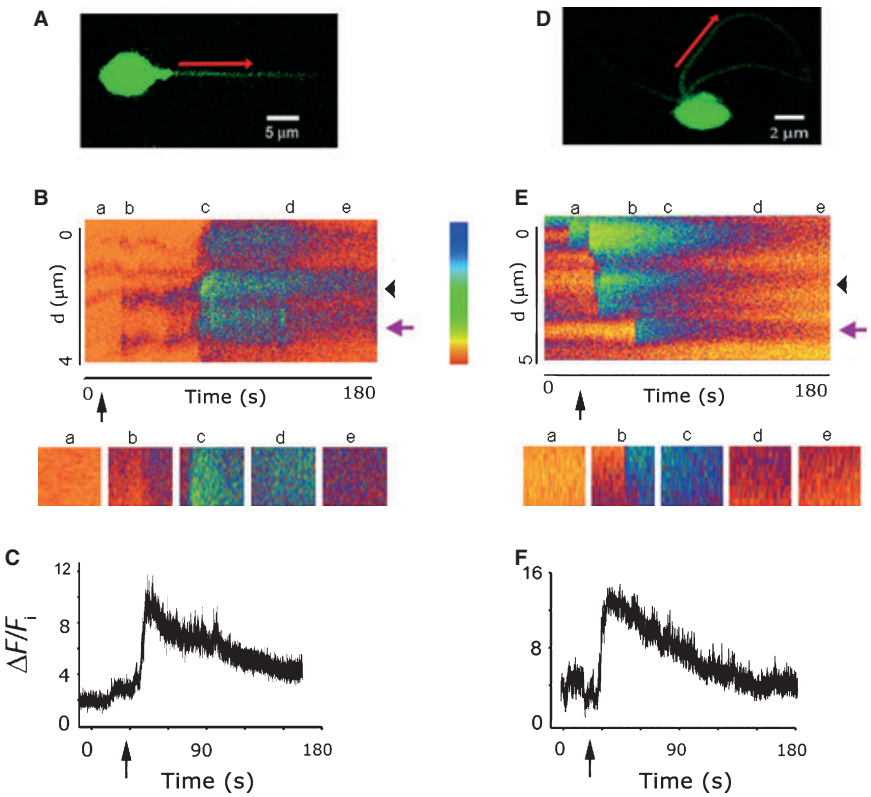

FIG. 2. Effects of inhibiting PMCA and NCX on Ca^{2+} microdomains and Ca^{2+} clearance. (A) Olfactory receptor neuron incubated in 50 μM CE to inhibit PMCA, with the red arrow indicating the olfactory cilia segment studied and the direction of the scan. (B) Ca^{2+} fluorescence changes along the cilia. (C) Time course of the fluorescence change for a selected region in the cilium. $\tau_{0.5}$ = 34 s. (D) Ciliary segment of another olfactory neuron examined under Li^{+}-Ringer's solution to abolish NCX activity. (E) Fluorescence change as a function of distance and time. (F) Time course of fluorescence decay; $\tau_{0.5}$ = 31 s. Labels as in Fig. 1.

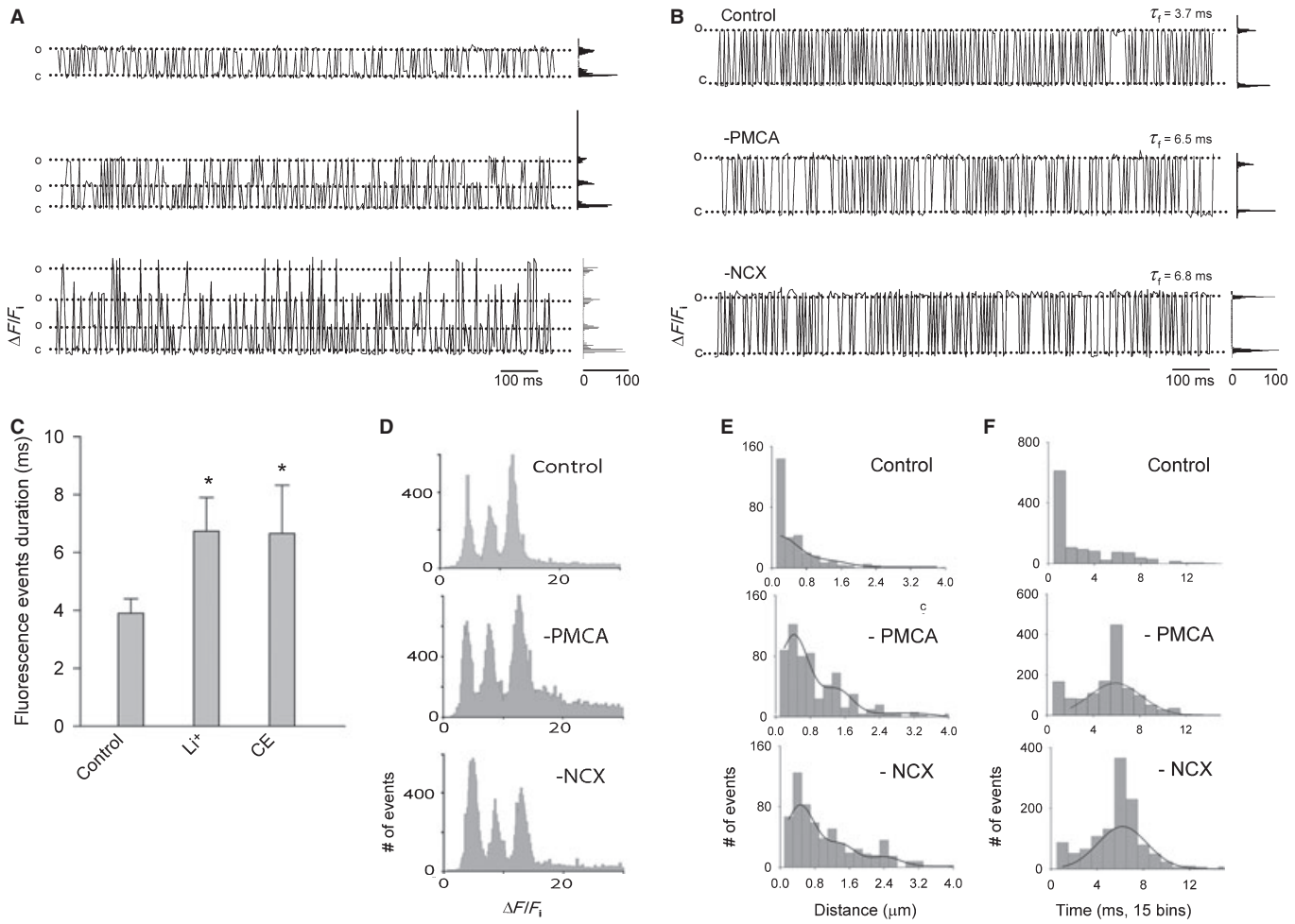

FIG. 3. Unitary Ca^{2+} events recorded in olfactory cilia. (A) Fluorescence recordings from three spots, exhibiting one, two and three amplitude levels. Fluorescence changes were normalized by dividing the change in fluorescence (ΔF) by the average basal fluorescence before the UV flash (F_i). The *y*-scale has been arbitrarily scaled so that the change in fluorescence to the first level is the same for the three traces. (B) Representative high-resolution fluorescence recordings from three individual spots of different cilia under different condition: Control is normal Ringer's, −PMCA is Ringer's with 50 μM CE and −NCX is Li^+-Ringer's. (C) Plot showing the average durations of the fluorescence events under each condition; measurements from five spots each (mean ± SD; control vs. Li^+, $F = 8$, $t = -3.50$, $P = 0.008$; control vs. CE, $F = 8$, $t = -4.96$, $P = 0.001$; Student's test). (D) Fluorescence intensity histograms for different conditions, each one comprising spots obtained from multiple cilia. (E) Histograms showing the cumulative distribution of the spatial dimension of the fluorescence events induced by UV light for the different conditions, fitted with Gaussian functions. (F) Histograms showing the cumulative distribution of the duration of the fluorescence events under the different conditions, fitted with Gaussian functions.

external Ca^{2+} is the origin of intraciliary Ca^{2+} increments. Thus, we refer to the cAMP-induced discrete fluorescence increases as 'Ca^{2+} microdomains'. We noticed the existence of a basal frequency of fluorescence events preceding the UV flash, which may be attributed to the low spontaneous activity of the CNG channels (Kleene, 2000).

Inhibition of either of two Ca^{2+} transporters slowed down the recovery of luminal Ca^{2+} level (Fig. 2), in accordance with the slackening in the relaxation of the Cl_{Ca} transduction current by these pharmacological agents (Castillo *et al.*, 2007). In the presence of the PMCA blocker CE (50 μM), ciliary fluorescence (Fig. 2A) increased at discrete sites with a more diffuse distribution than in control conditions (Fig. 2B) and relaxed more slowly (Fig. 2C; $\tau_{0.5} = 34$ s; average $\tau_{0.5} = 30.18 \pm 6.4$ s; $n = 8$ of 14 cells tested). Abolishing NCX activity by substituting external Na^+ with Li^+ (Fig. 2D–F) resulted in more diffuse microdomains (Fig. 2E) and affected fluorescence decline in a similar way as seen with inhibition of PMCA (Fig. 2F; $\tau_{0.5} = 31$ s; average $\tau_{0.5} = 28.12 \pm 5.20$ s; $n = 6$ of 11 cells tested). This evidence supports the contribution of both transporters to Ca^{2+} clearance.

A close examination of the recordings revealed that the evoked Ca^{2+} response was composed of brief, discrete events (Fig. 1B, insets). Strikingly, inspection of such individual fluorescence events as a function of time revealed the occurrence of square fluctuations between a small number (one to three, depending on the spot) of well-defined and regularly spaced amplitude levels, closely resembling single-channel events, suggesting a stereotyped organization of CNG channels in the ciliary membrane (Fig. 3A). Respective amplitude distributions are shown besides each trace. The recordings chosen for this type of analysis correspond to those in which separate events were discernible within the fluorescence activity; we obtained recordings where this was not possible because of excessive activity (not shown), which might reflect a higher spot density as a result of the higher cAMP levels attained in such experiments.

Traces from spots containing one individual channel, each from the three experimental conditions tested (control, PMCA inhibited and NCX inhibited), are shown in Fig. 3B. As in control conditions, levels ranged from one to three under the different treatment

conditions. The average duration of the fluorescence events (τ_f) for the control trace was 3.7 ms. This value increased by nearly 50% upon abolition of either PMCA or NCX (τ_f = 6.5 and 6.8 ms, respectively). Average τ_f values for each condition [3.9 ± 0.5 ms, 6.7 ± 1.2 ms and 6.7 ± 1.7 ms, respectively (mean ± SD); control vs. Li^+, $F = 8$, $t = -3.50$, $P = 0.008$; control vs. CE, $F = 8$, $t = -4.96$, $P = 0.001$; Student's test) are plotted in Fig. 3C. Figure 3D depicts fluorescence amplitude histograms, each of which was built with data obtained from several cilia (see figure legend), recorded under the different experimental conditions. Remarkably, all histograms display three equally spaced peaks, suggesting the presence of events with three well-defined fluorescence amplitudes above the basal fluorescence level. We examined the spatial dimension of the fluorescence spots, for which we plotted the cumulative distribution of the event sizes (Fig. 3E). The events recorded under control condition were of a size at the limit of resolution of the microscope (approximately 0.2 μm). However, the width of the spots widened when either transporter was abolished, the average widths being 0.4 ± 0.5 μm in CE and 0.4 ± 0.3 μm in Li^+ solution. The cumulative distribution of the duration of the events under control conditions showed an average value below the time resolution of the instrument (< 2 ms), whereas it increased to 6.3 ± 3.8 ms when PMCA was abolished and to 6.9 ± 3.2 ms when NCX was abolished (Fig. 3F).

Discussion

In this work, we determined the existence of Ca^{2+} microdomains comprising a small number of CNG channels in olfactory cilia, and investigated Ca^{2+} dynamics following sudden uniform increments in intraluminal concentrations of cAMP, confirming the participation of both NCX and PMCA in Ca^{2+} clearance.

The relaxation kinetics of the fluorescence increment are comparable to those previously observed with regular confocal microscopy in odor-stimulated salamander olfactory cilia (approximately 7.7 s) (Leinders-Zufall *et al.*, 1998). However, the latency of the Ca^{2+} fluorescence events following UV illumination in our experiments (5–15 s) was much longer than that of the whole cell current induced by photoreleased cAMP (approximately 0.1 s) (Takeuchi & Kurahashi, 2002; Castillo *et al.*, 2007), its principal component being the Cl_{Ca} current. Its relaxation time (approximately 11 s) was much longer than that of the current (< 1 s) as well. Our experiments do not allow us to unravel the reason for the unexpectedly long latency. One possibility is that the whole cell current, mainly carried by Cl^- ions, directly depends on the free Ca^{2+} concentration at the internal membrane surface, which is sensed by the Cl_{Ca} channels located immediately next to the open CNG channels in the microdomain (these can be as close as 20 nm). Thus, a large electrical signal rapidly develops as the Ca^{2+} concentration reaches the threshold for Cl_{Ca} channel activation, as a result of the high Ca^{2+} sensitivity of the Cl^- channels (nanomolar) and the important amplification of this last transduction step. If the Ca^{2+} change occurs in the vicinity of the ion channels (within 20 nm), it does not necessarily translate into a fluorescence change, because of the very weak fluorescence signal that it would evoke. In contrast, the latency preceding the detectable Ca^{2+} fluorescence events is much longer because, in spite of the fact that cAMP rises uniformly in the entire ciliary lumen, it drops very quickly to subthreshold levels within the miniscule microdomain compartments, which contain most ciliary PDE molecules (Cygnar & Zhao, 2009). The strong PDE barrier would greatly limit cAMP diffusion from the luminal pool to the microdomain, where its concentration would gradually increase to eventually reach the threshold for CNG activation. The time that this takes depends on the concentration of cAMP at the lumen and the potency of the PDE barrier. In the present work, this latency was several seconds to tens of seconds. Interestingly, Kurahashi (1990) observed that the latency of the whole cell current evoked by introducing a large concentration of cAMP (0.5 mM) with a patch pipette positioned at the base of the dendrite was much longer (1.4 s) than that evoked with the patch pipette positioned at the dendritic knob (0.2 s). In our experiments, we are not aware of the caged-cAMP concentration attained in the cell after incubation in the caged compound (250 μM), or the concentration of photoreleased cAMP, but they may have been much < 0.5 mM. Accordingly, it does not seem unreasonable that the fluorescence event activity was preceded by long delays.

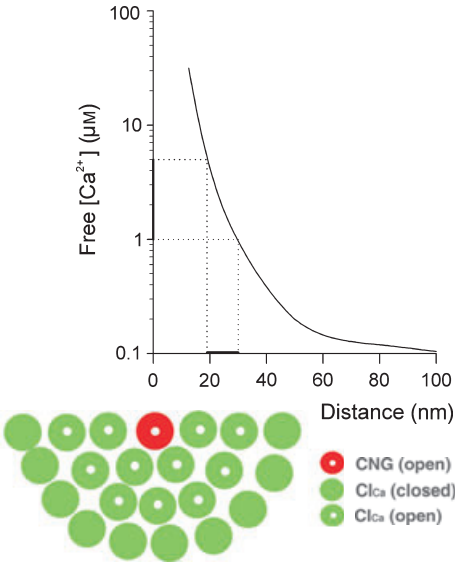

FIG. 4. Model of an olfactory cilium transducisome. The model depicts one transducisome (actually half of it, for convenience) as suggested by our results, next to the profile of free Ca^{2+} concentration as a function of distance from the mouth of a single Ca^{2+}-permeant channel, in this case a CNG channel; adapted from Naraghi & Neher (1997). The CNG channel is surrounded by multiple Cl_{Ca} channels, whose only Ca^{2+} source is the CNG channel. The $K_{0.5}$ range of Cl_{Ca} for Ca^{2+}, 1–5 μM (Kleene & Gesteland, 1991; Reisert *et al.*, 2003), is indicated by a bar beside the ordinate, projected to the distance axis. Proteins have been assigned an estimated size of approximately 10 nm (Fakler & Adelman, 2008). According to the model, [Ca^{2+}] drops below the threshold for Cl_{Ca} activation beyond the second row of proteins surrounding the CNG channel, implying that if there were further Cl_{Ca} channels in the transducisome, they could not open. As the Ca^{2+} transporters and protein constituents of the transduction cascade are likely to be part of the transducisome as well, the number of Cl_{Ca} channels within the restricted transducisome area may be even smaller.

Regarding the relaxation of the responses to photorelease cAMP, we would expect the nucleotide to rapidly decline within the microenvironment surrounding the CNG channels because of potent local PDE activity, explaining the relatively low relaxation time of the Cl^- current. However, the cAMP concentration in the bulk of the cilium would take a much longer time to decline, because the PDE molecules that hydrolyze it are confined to the membrane and are likely to become overwhelmed by the abnormally large amounts of cAMP generated by the photolysis. This is manifested by the slowly developing but sustained activity of discrete fluorescence events. Eventually, cAMP drops to basal levels, ending the fluorescence events.

Besides the striking similarities in appearance between the Ca^{2+} fluorescence fluctuations and the single CNG channel activity

recorded electrically in patches excised from the dendritic knob, the dwell time obtained from the fluorescence measurements is close to that derived from electrical measurements (dwell time (τ_o) = ~1.5 ms) (Zufall *et al.*, 1991), with substantially higher time resolution (2.5 vs. approximately 0.3 kHz), indicating that the fluorescence events are manifestations of highly localized Ca^{2+} increments occurring as individual CNG channels open in one microdomain. The fluorescence levels indicate the number of CNG channels contained in individual microdomains. The prolongation of the dwell time occurring upon abolition of PMCA or NCX can be explained by the retention of Ca^{2+} around the channel for a longer time, consistent with the participation of both transporters in ciliary Ca^{2+} removal.

A recent study showed that identical cAMP increments evoked in successive 1-μm segments of individual olfactory cilia induced electrical responses of similar amplitudes, leading to the conclusion that CNG channels were uniformly located along the cilium (Takeuchi & Kurahashi, 2008). However, our finding of < 0.2-μm Ca^{2+} microdomains suggest that if several of them were activated within a 1-μm ciliary segment, the resulting electrical responses to identical stimuli would be alike. The existence of microdomains was questioned by Reisert *et al*. (2003), on the basis of studies with inside-out patches excised from dendritic knobs, some of which might have additionally contained cilia. From cAMP-evoked multichannel Cl^- currents recorded at various Ca^{2+} buffer concentrations, they concluded that CNG and Cl_{Ca} channels were approximately 120 nm apart, a distance incompatible with co-localization into a transducisome. However, there is no reason to expect a similar molecular organization or spatial distribution of channels in the cilia and knob membranes, nor there is any evidence that the Cl_{Ca} channels in the knob are the same as those in the cilia.

The small number of CNG channels in the microdomains suggests that the odor transduction cascade involves low amplification, where the odor molecule binding to a single receptor would lead to the opening of very few (typically three or fewer) CNG channels and a limited number of Cl_{Ca} channels surrounding each CNG in discrete sparse microdomains. This result is in agreement with the notion that, at low concentration, odor responses are the linear summation of multiple elementary responses of extremely small amplitude (Bhandawat *et al.*, 2005). This observation is based on the statistical analysis of responses to brief odorant stimuli of low concentration, where the dose–response relationship was evidently linear. A key consideration was that the odor receptor–G_{olf} interaction time is brief (approximately 0.1 ms), implying that an odor receptor has a low probability of activating one G_{olf} protein when it binds an odor molecule. On the other hand, as for other Ca^{2+}-conducting channels, a pronounced Ca^{2+} profile around a CNG channel limits to tens of nanometers from the mouth of this channel the distance at which the Ca^{2+} concentration is sufficient for Cl_{Ca} activation (Naraghi & Neher, 1997; Bauer, 2001). Therefore, it is reasonable to postulate that the CNG and the Cl_{Ca} channels will localize to the Ca^{2+} microdomains, and that the number of Cl_{Ca} channels that can be housed and be functional within the microdomain cannot be large. Assuming that most of the area immediately surrounding a CNG where the Ca^{2+} concentration attains the threshold for Cl_{Ca} activation is occupied by Cl_{Ca} channels and a few transporter molecules, and a diameter of these proteins of 10 nm (Long *et al.*, 2005; Fakler & Adelman, 2008), fewer than 10 Cl_{Ca} channels would fit in such area. Beyond this area, Ca^{2+} increments would be insufficient to open Cl_{Ca} channels (Fig. 4). This conclusion has an important implication regarding the characteristics of the Cl_{Ca} channel currently under debate (Frings *et al.*, 2000; Kleene, 2009). As the Cl^- current associated with a single CNG channel is three to four times the cationic current (Lowe & Gold, 1993), the number of Cl_{Ca} channels in a microdomain must be sufficient to allow such anionic current, but it cannot exceed the number of channels that can sterically fit within it. This number is directly related to the single Cl_{Ca} channel conductance; if its conductance were 1 pS (Reisert *et al.*, 2003; Pifferi *et al.*, 2006, 2009; Stephan *et al.*, 2009), and as one CNG channel conducts 0.08 pA at −55 mV (Zufall & Firestein, 1993), five or six Cl_{Ca} channels would be required to conduct 0.32 pA, in agreement with the model of Fig. 4. This implies that, under physiological conditions, an elementary response would be undetectable, and several such responses would have to occur simultaneously in the cilia of an olfactory neuron to be physiologically significant. This is in agreement with the notion that vertebrate olfactory receptor neurons are incapable of responding to individual odor molecules (Paysan & Breer, 2001). Interestingly, elements capable of sustaining macromolecular complexes exist in olfactory cilia, such as scaffolding proteins (Saavedra *et al.*, 2008) and lipid rafts (Schreiber *et al.*, 2000), although it is still unclear whether they play such a role.

The duration and width of the microdomains were similarly increased when either of the two Ca^{2+} transporters present in the olfactory cilia was abolished. These observations imply that NCX and PMCA effectively contribute to limit the diffusion of Ca^{2+} away from the CNG channels, suggesting that they localize in close proximity to the CNG channels, probably being part of the microdomain. This would ensure efficient removal of Ca^{2+} ions after the transduction machinery is activated.

In conclusion, our data show that Ca^{2+} increments in olfactory cilia that result from CNG channel opening are confined to microdomains. Each microdomain comprises one to three CNG channels. It seems likely that these channels are associated with other transduction proteins to form transducisomes, giving rise to elementary odor responses that add up to generate the cellular odor response. In addition, the present results strongly support the involvement of both NCX and PMCA in the extrusion of Ca^{2+} and in the restriction of Ca^{2+} increases in olfactory cilia.

Acknowledgements

We thank Magdalena Sanhueza and Ricardo Delgado for discussions on early versions of this article. This work was supported by grant TW007920 from the Fogarty International Center of the NIH (J. Bacigalupo and D. Restrepo), NIDCD grants DC006070 and DC04657 (D. Restrepo), MIDEPLAN ICM-P05-001-F (J. Bacigalupo), FONDECYT 1080653 (J. Bacigalupo), a MECESUP UCH0409 training research fellowship (K. Castillo), the Graduate Department and Academic Affairs, University of Chile (K, Castillo) and a CONICYT doctoral fellowship (K. Castillo).

Abbreviations

CE, 5(6)-carboxyeosin diacetate, succinimidyl ester; Cl_{ca}, Ca^{2+}-activated Cl^-; CNG, cyclic nucleotide-gated; F_i, basal average fluorescence intensity in the same ciliary segment before exposure of the cilium to the UV light flash; Fluo-4 AM, fluo-4 acetoxymethyl ester probe; NCX, Na^+/Ca^{2+} exchanger; PDE, phosphodiesterase; PMCA, plasma membrane Ca^{2+}-ATPase; SD, standard deviation; ΔF, fluorescence intensity at any time point minus the basal average fluorescence intensity in the same ciliary segment before exposure of the cilium to the UV light flash; $\tau_{0.5}$, time at which the Ca^{2+} signal declined to half its peak value; τ_f, average duration of fluorescence events.

References

Antolin, S., Reisert, J. & Matthews, H.R. (2010) Olfactory response termination involves Ca^{2+}-ATPase in vertebrate olfactory receptor neuron cilia. *J. Gen. Physiol.*, **135**, 367–378.

Bauer, P.J. (2001) The local Ca concentration profile in the vicinity of a Ca channel. *Cell Biochem. Biophys.*, **35**, 49–61.
Bhandawat, V., Reisert, J. & Yau, K.W. (2005) Elementary response of olfactory receptor neurons to odorants. *Science*, **308**, 1931–1934.
Castillo, K., Delgado, R. & Bacigalupo, J. (2007) Plasma membrane Ca(2+)-ATPase in the cilia of olfactory receptor neurons: possible role in Ca(2+) clearance. *Eur. J. Neurosci.*, **26**, 2524–2531.
Chen, T.Y. & Yau, K.W. (1994) Direct modulation by Ca(2+)-calmodulin of cyclic nucleotide-activated channel of rat olfactory receptor neurons. *Nature*, **368**, 545–548.
Cygnar, K.D. & Zhao, H. (2009) Phosphodiesterase 1C is dispensable for rapid response termination of olfactory sensory neurons. *Nat. Neurosci.*, **12**, 454–462.
Demuro, A. & Parker, I. (2006) Imaging single-channel calcium microdomains. *Cell Calcium*, **40**, 413–422.
Denk, W. & Svoboda, K. (1997) Photon upmanship: why multiphoton imaging is more than a gimmick. *Neuron*, **18**, 351–357.
Denk, W., Holt, J.R., Shepherd, G.M. & Corey, D.P. (1995) Calcium imaging of single stereocilia in hair cells: localization of transduction channels at both ends of tip links. *Neuron*, **15**, 1311–1321.
Fakler, B. & Adelman, J.P. (2008) Control of K(Ca) channels by calcium nano/microdomains. *Neuron*, **59**, 873–881.
Frings, S., Reuter, D. & Kleene, S.J. (2000) Neuronal Ca^{2+}-activated Cl^- channels – homing in on an elusive channel species. *Prog. Neurobiol.*, **60**, 247–289.
Kleene, S.J. (2000) Spontaneous gating of olfactory cyclic-nucleotide-gated channels. *J. Membr. Biol.*, **178**, 49–54.
Kleene, S.J. (2009) Identifying olfaction's 'other channels'. *J. Physiol.*, **587**, 4135–4136.
Kleene, S.J. & Gesteland, R.C. (1991) Calcium-activated chloride conductance in frog olfactory cilia. *J. Neurosci.*, **11**, 3624–3629.
Kurahashi, T. (1990) The response induced by intracellular cyclic AMP in isolated olfactory receptor cells of the newt. *J. Physiol.*, **430**, 355–371.
Kurahashi, T. & Yau, K.W. (1993) Co-existence of cationic and chloride components in odorant-induced current of vertebrate olfactory receptor cells. *Nature*, **363**, 71–74.
Leinders-Zufall, T., Greer, C.A., Shepherd, G.M. & Zufall, F. (1998) Imaging odor-induced calcium transients in single olfactory cilia: specificity of activation and role in transduction. *J. Neurosci.*, **18**, 5630–5639.
Long, S.B., Campbell, E.B. & Mackinnon, R. (2005) Crystal structure of a mammalian voltage-dependent Shaker family K^+ channel. *Science*, **309**, 897–903.
Lowe, G. & Gold, G.H. (1993) Nonlinear amplification by calcium-dependent chloride channels in olfactory receptor cells. *Nature*, **366**, 283–286.
Menco, B. (1992) Ultrastructural studies on membrane, cytoskeletal, mucous, and protective compartments in olfaction. *Microsc. Res. Tech.*, **22**, 215–224.
Naraghi, M. & Neher, E. (1997) Linearized buffered Ca^{2+} diffusion in microdomains and its implications for calculation of $[Ca^{2+}]$ at the mouth of a calcium channel. *J. Neurosci.*, **17**, 6961–6973.
Paysan, J. & Breer, H. (2001) Molecular physiology of odor detection: current views. *Pflugers Arch.*, **441**, 579–586.
Pifferi, S., Pascarella, G., Boccaccio, A., Mazzatenta, A., Gustincich, S., Menini, A. & Zucchelli, S. (2006) Bestrophin-2 is a candidate calcium-activated chloride channel involved in olfactory transduction. *Proc. Natl Acad. Sci. USA*, **103**, 12929–12934.
Pifferi, S., Dibattista, M. & Menini, A. (2009) TMEM16B induces chloride currents activated by calcium in mammalian cells. *Pflugers Arch.*, **458**, 1023–1038.
Reisert, J. & Matthews, H.R. (1998) Na^+-dependent Ca^{2+} extrusion governs response recovery in frog olfactory receptor cells. *J. Gen. Physiol.*, **112**, 529–535.
Reisert, J., Bauer, P.J., Yau, K.W. & Frings, S. (2003) The Ca-activated Cl channel and its control in rat olfactory receptor neurons. *J. Gen. Physiol.*, **122**, 349–363.
Saavedra, M.V., Smalla, K.H., Thomas, U., Sandoval, S., Olavarria, K., Castillo, K., Delgado, M.G., Delgado, R., Gundelfinger, E.D., Bacigalupo, J. & Wyneken, U. (2008) Scaffolding proteins in highly purified rat olfactory cilia membranes. *Neuroreport*, **19**, 1123–1126.
Schild, D. & Restrepo, D. (1998) Transduction mechanisms in vertebrate olfactory receptor cells. *Physiol. Rev.*, **78**, 429–466.
Schreiber, S., Fleischer, J., Breer, H. & Boekhoff, I. (2000) A possible role for caveolin as a signaling organizer in olfactory sensory membranes. *J. Biol. Chem.*, **275**, 24115–24123.
Shuai, J. & Parker, I. (2005) Optical single-channel recording by imaging Ca^{2+} flux through individual ion channels: theoretical considerations and limits to resolution. *Cell Calcium*, **37**, 283–299.
Stephan, A.B., Shum, E.Y., Hirsh, S., Cygnar, K.D., Reisert, J. & Zhao, H. (2009) ANO2 is the cilial calcium-activated chloride channel that may mediate olfactory amplification. *Proc. Natl Acad. Sci. USA*, **106**, 11776–11781.
Takeuchi, H. & Kurahashi, T. (2002) Photolysis of caged cyclic AMP in the ciliary cytoplasm of the newt olfactory receptor cell. *J. Physiol.*, **541**, 825–833.
Takeuchi, H. & Kurahashi, T. (2008) Distribution, amplification, and summation of cyclic nucleotide sensitivities within single olfactory sensory cilia. *J. Neurosci.*, **28**, 766–775.
Zufall, F. & Firestein, S. (1993) Divalent cations block the cyclic nucleotide-gated channel of olfactory receptor neurons. *J. Neurophysiol.*, **69**, 1758–1768.
Zufall, F., Firestein, S. & Shepherd, G.M. (1991) Analysis of single cyclic nucleotide-gated channels in olfactory receptor cells. *J. Neurosci.*, **11**, 3573–3580.